

Investigating Noise Reduction in an Octave-Spanning Ti:Sapphire Laser

by

Annemarie N. Grandke

Submitted to the Department of Physics in partial fulfillment of the requirements
for the Degree of

Bachelor of Science

at the

MASSACHUSETTS INSTITUTE OF TECHNOLOGY

June 2004

© Annemarie N. Grandke 2004

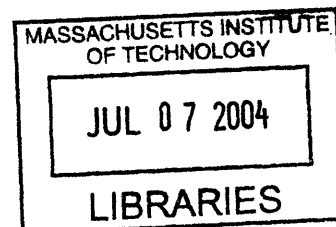
All rights reserved.

The author hereby grants to MIT permission to reproduce and to distribute publicly paper and electronic copies of this thesis document in whole or in part.

Author _____
Department of Physics
May 7, 2004

Certified by _____
Thomas J. Greytak
Professor
Thesis Supervisor

Accepted by _____
David E. Pritchard
Senior Thesis Coordinator, Department of Physics



ARCHIVES

Contents

1	Introduction	7
2	Carrier-Envelope Phase of Short Pulses	9
2.1	Evolution of the Carrier-Envelope Phase.....	9
2.2	Frequency Domain Description of Carrier-Envelope Phase Evolution in a Pulse Train.....	11
2.3	Stabilization of the Frequency Comb.....	13
3	Description of the System and Experimental Setup	17
3.1	The System.....	17
3.2	Experimental Setup.....	21
4	Measurements and Results	25
4.1	Noise reduction.....	25
4.2	Beam Characterization.....	28
5	Conclusion and Future Research	31

List of Figures

2-1	Pulse Schematic. $\Delta\varphi$ is the phase slip between successive pulses. T denotes the pulse round trip time in the cavity.....	10
3-1	Schematic diagram of octave-spanning prism-less laser. Gray and black mirrors are type I and II DCMs respectively. The BaF ₂ wedges are used for fine-tuning the dispersion [1].....	17
3-2	Measured output spectrum (solid line) for 80 MHz repetition rate laser. The octave is reached at approximately 25 dB of the average power level. The average mode-locked power is 90 mW. Also shown is the OC transmission curve (dashed line) for the ZnSe/MgF ₂ Bragg-stack, which has approximately 1% transmission at 800 nm [1].....	18
3-3	Setup for f_{ceo} detection and lock. Main components of the system include the laser itself, the self-referencing f-2f interference setup, and the active feedback and stabilization electronics [1].....	20
3-4a	The Noise Eater apparatus. Note that the Electro-optical crystal is a polarization rotator.....	22
3-4b	The Noise Eater feedback system. The detected signal from the beam splitter is compared to a reference signal in the feedback electronics, and a bias voltage is applied to the electro-optic crystal.....	22
3-5	The experimental set up for testing the EOM performance as a pump power noise eater. The half-waveplate is used to make polarization adjustments. The pair of folding mirrors in front of the EOM is used for optimization of the laser beam transmission through the EOM.....	24
4-1	Spectral densities of the phase error signal at the output of the digital phase detector for the f_{ceo} lock (solid line) with scale on the left. Spectral density of the pump noise (dash-dotted line) and system noise floor (dotted line), with	

scale on the right. The major contribution to f_{ceo} noise is due to pump noise [1].....	25
4-2 Spectral Density Measurements of the pump noise without (dashed line) and with (solid line) the EOM in operation. The dotted line is the system noise floor.....	27
4-3 Transmission of power through the EOM as a function of beam size. Clearly, as the beam size becomes smaller, more power can be transmitted through the EOM, indicating that the beam is no longer distorted or clipping because it is too large for the aperture.....	29
4-4 Beam size transmission as a function of power transmission. As the EOM transmits a higher percentage of the incident power, the quality of the laser beam transmitted, defined by (incident beam size)/(exiting beam size), also improves.....	30
4-5 Graphical estimate of the maximum beam size for optimum EOM operation at a pump power of 0.5 W.....	30

Chapter 1

Introduction

Over the past few years, the marriage between cw based ultraprecision laser work and ultrafast femtosecond lasers has produced tremendous scientific progress in both areas. Applications in optical frequency metrology and optical clocks, as well as coherent control and optical waveform synthesis have been investigated [2-4]. Of special significance to frequency metrology has been the generation of frequency combs based on femtosecond lasers. These optical combs consist of pulse trains which exhibit rigorous periodicity in the spectral domain and which are generated by mode-locked femtosecond lasers. Traditionally, the spectral width of these frequency combs produced from mode-locked lasers has had to be broadened, while at the same time maintaining the mode spacing, through self phase modulation in the nonlinear medium of microstructure fibers [5]. Recently, however, an octave-spanning prismless Ti:sapphire laser has been demonstrated by using special double-chirped mirror pairs which provide compact dispersion compensation, hence allowing for the spectrum to be generated directly from the laser itself without launching the pulse train into a microstructure fiber [6]. An octave spanning frequency comb is necessary to employ a 1f-2f carrier-envelope offset frequency stabilization scheme which allows for control of the carrier-envelope phase and the establishment of phase coherence among individual components of the comb [1].

It is exactly this control of the carrier envelope offset frequency, f_{ceo} , which is crucial for optical metrology. It is hence extremely desirable to construct an optimized control

scheme for the optical comb which allows for maximum stabilization of f_{ceo} through a feedback loop. Phase spectral density (PSD) measurements have shown that f_{ceo} noise after stabilization is directly correlated to pump noise, and hence limited by it [1]. Physically, this is caused by non-linear effects in the crystal. The index of refraction of the crystal contains a second order term dependent on intensity, I , of the pump laser. Since the phase of the carrier-envelope, φ , depends on the index of refraction of the crystal, the carrier envelope offset frequency f_{ceo} is related to the intensity, and consequently f_{ceo} noise is connected to pump noise. Hence, a pre-stabilization of pump power amplitude noise is desirable in order to obtain a less noisy carrier envelope offset frequency.

This thesis investigates possible methods of decreasing pump power amplitude noise with the overall goal of improving the stabilization of f_{ceo} . A commercially manufactured noise eater, consisting of an electro-optical modulator (EOM) and feedback electronics is employed to cancel the pump power noise through a feedback-control system. This method of noise control is very effective. Upon achieving a noise reduction of 20 dB with the noise eater, further measurements were made with a beam profiler to determine the ideal aperture size required for optimizing the noise reduction performance.

Chapter 2

Carrier-Envelope Phase of Short Pulses

The phase of an electromagnetic field has traditionally not been a physically meaningful quantity, because most measurements in optics are done with intensity [7]. It has recently become possible, by using the envelope of a pulse as a phase reference, to control the phase of the electromagnetic field of ultrashort pulses [8]. Denoting the electric field of a laser pulse by

$$E(t) = A(t) \cos(\omega_1 t + \varphi) \quad (1)$$

then φ determines the carrier-envelope phase. For a pulse train emitted by a modelocked laser, there will be a pulse-to-pulse change in φ , which may be denoted as $\Delta\varphi$. While it has been possible to control and measure $\Delta\varphi$, similar control over φ itself has not yet been achieved.

2.1 Evolution of the Carrier-Envelope Phase

Ultrashort optical pulses are generated by modelocked lasers through fixing the relative phases of all of the lasing longitudinal modes [9]. The larger the bandwidth over which mode-locking techniques can be applied, the shorter are the resulting pulses that can be produced by such mode-locked lasers. When dealing with extremely short pulses, often on the order of a few femtoseconds, the relative phase between the underlying electric field carrier wave and the peak of the pulse envelope becomes important.

For any material except vacuum, dispersion will result in differing phase and group velocities of the pulse train and cause φ to evolve rapidly between successive pulse envelope peaks. It is dispersion inside the material components of the laser cavity, including the Ti:sapphire crystal and the BaF₂ wedges, which causes many cycle slips of the envelope during propagation in the cavity and the overall evolution of the phase. Since φ evolves during propagation inside the cavity of a modelocked laser, each pulse in the emitted pulse train will increment by an amount $\Delta\varphi$ (Figure 2-1). For many experiments, controlling $\Delta\varphi$ and producing a pulse train of constant φ is an essential prerequisite.

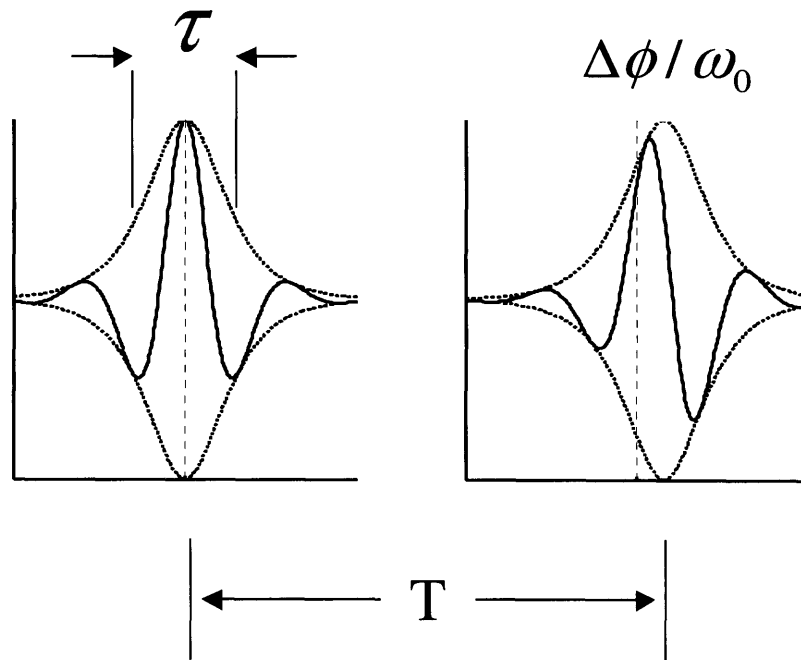


Figure 2-1: Pulse Schematic. $\Delta\varphi$ is the phase slip between successive pulses. T denotes the pulse repetition rate.

Commonly, time domain methods have been employed to control the phase of femtosecond pulses [10]. However, because these methods do not make use of active feedback, rapid dephasing between pulses can occur. Through actively controlling the carrier-envelope phase in the frequency domain, a stable pulse-to-pulse phase relation can be ensured [9].

2.2 Frequency Domain Description of Carrier-Envelope Phase Evolution in a Pulse Train

On a spectrometer, the spectrum of a modelocked laser will appear as a broad, continuous spectrum. The spectrum of the individual pulses is given by this. If the resolution of the spectrometer were high enough, one would discover that the broad spectrum actually consists of a comb of optical frequencies [7]. If one performs a Fourier analysis of a train of identical pulses, it is revealed that the frequency spectrum is a comb in which the comb frequencies are integer multiples of f_{rep} , in other words, the interval between adjacent frequencies of the comb is defined by the pulse repetition rate [7].

Following the intuitive treatment of Reichert *et al* [5], the electric field of a mode-locked laser is given by

$$E(t) = \sum_{q=-\infty}^{+\infty} A_q e^{2\pi(f_c + qf_{rep})t} + c.c \quad (2)$$

where $A(t)$ is a strictly periodic envelope function, and hence expressible as a Fourier series in f_{rep} , and f_c is the optical carrier frequency. The spectrum of the electric field given by Equation 2 represents a comb of laser frequencies precisely spaced by the pulse repetition rate, f_{rep} , whose uniform spacing is a result of the periodicity of the envelope function $A(t)$ [5]. However, because the envelope of a circulating pulse travels with the group velocity v_g while the carrier phase has its own phase velocity v_p , and generally $v_g \neq v_p$, the carrier frequency f_c and therefore the frequency of each mode f_n is not simply and integer multiple of the pulse repetition rate [5]. Rather, in the frequency domain, the comb is offset from the integer multiples of f_{rep} by an offset frequency f_{ceo} [9].

To understand the connection between the pulse-to-pulse carrier envelope phase shift, $\Delta\phi$, and the absolute frequency spectrum, consider, as outlined by Jones *et al* [9], that the spectrum of a mode-locked laser consists of a temporal train of pulses. By using Fourier

transforms, it is easily shown that a shift in time corresponds to a phase shift linear with frequency [5]. Successive pulses will interfere within a narrow spectral bandwidth [9]. Only at those frequencies at which the pulses interfere constructively will a signal be observed; the condition for this is that the pulses have a phase shift of $2n\pi$, and if the pulse repetition time is denoted by T , the frequencies of constructive interference are given by $f_n = n/T = nf_{rep}$, where n is an integer and $T = f_{rep}^{-1}$ [9].

Considering now that the carrier envelope phase relative to the envelope changes from pulse to pulse by $\Delta\varphi$, there will be a shift in the frequencies of the comb. Since the condition for constructive interference again is that the phase difference be equal to $2n\pi$, the optical frequencies of the comb lines are thus given by [9]

$$f_n = nf_{rep} + f_{ceo}. \quad (3)$$

The comb of laser frequencies is thus shifted by an offset frequency f_{ceo} from the integer multiples of f_{rep} given by [5]

$$f_{ceo} = \frac{\Delta\varphi}{2\pi} T^{-1} = \frac{\Delta\varphi}{2\pi} f_{rep}. \quad (4)$$

Thus, it can be seen that the pulse-to-pulse phase evolution causes a rigid shift of the frequency comb from simple integer multiples of the repetition rate by f_{ceo} [7]. Thus $\Delta\varphi$ may be determined if f_{ceo} can be measured.

To summarize, a mode-locked laser produces one pulse per cavity round trip. Since the carrier slips through the envelope as the pulse circulates in the cavity, what determines f_{ceo} is thus the overall accumulated carrier phase, with respect to the envelope, for each round trip. Most generally, the phase and frequency offsets in a free-running laser are completely arbitrary, and usually subject to a time drift, because the phase-group velocity difference is not constant over time. If the accumulated carrier phase is a integer multiple of 2π , there will

be no offset, because there is no pulse-to-pulse phase shift for the emitted pulses and the frequencies are all integers multiples of the repetition rate [9].

2.3 Stabilization of the Frequency Comb

Frequency combs are important in both optical metrology and atomic clocks. However, for the frequency comb to be an effective tool in these applications, it needs to be stabilized in the optical domain. The comb produced by a free-running laser will drift around in frequency space because of a phase-group velocity time drift. Furthermore, the spacing of the frequencies can vary, depending on the stability of the repetition rate of the laser, this phenomenon is called “breathing” of the comb. Thus if the optical frequencies of individual comb lines are given by $f_n = nf_{rep} + f_{ceo}$, then in order to stabilize the comb in frequency space, two degrees of freedom need to be controlled: the carrier-envelope offset frequency f_{ceo} and the pulse repetition rate f_{rep} .

Applications in Optical Metrology

The goal of optical metrology is to determine, to the highest possible accuracy, the frequencies of optical transitions. In the past, this has been accomplished by comparing these optical frequencies to a universal reference frequency, a hyperfine transition line in Cesium, on the order of 9 GHz. Via a frequency chain consisting of multiple diode lasers, one goes from the optical transition frequency in question, which is usually on the order of a few hundred THz, in incremental steps to the reference frequency [11]. However, since a frequency chain is specific to a certain optical transition, for each new optical measurement, a new frequency chain is needed. Hence a frequency comb, with its 1,000,000+ comb lines, covering most optical transition frequencies, represents a real advantage. By beating the unknown optical frequency with the frequencies of the optical comb and measuring the beat frequency, the optical frequency may be determined as follows if both f_{ceo} and f_{rep} are known:

$$f_{beat} = f_{comb} \otimes f_{opt} = f_{opt} - f_{comb} = f_{opt} - (nf_{rep} + f_{ceo}) \quad (5)$$

Although many beat frequencies will be produced when the optical frequency is beat against the comb lines, the smallest frequency is going to be the one between the optical frequency and the closest comb line, and can easily be measured.

$\Delta\phi$ manifests itself in the frequency domain as a rigid offset by f_{ceo} . As has been demonstrated, controlling the carrier-envelope phase, $\Delta\phi$, allows for direct control of the absolute frequencies of the optical comb, and vice versa [9]. It is thus crucial to have an accurate method of detecting and determining f_{ceo} , for in this manner $\Delta\phi$ may be controlled. Furthermore, to have a completely stabilized comb necessary for making precision measurements, the repetition rate f_{rep} also needs to be controlled and determined.

A convenient approach for determining f_{ceo} is to employ an elegant technique known as *self-referencing*. This technique produces f_{ceo} by comparing the low and high frequency ends of the spectrum of comb lines. In order to be able to make use of this method, an optical spectrum that spans a factor of 2 in frequency, known as an optical octave, is required [9]. Only if the spectrum is sufficiently broad to meet this condition will the second harmonic of the low frequency end of the spectrum overlap with the high frequency end. If the frequency of a comb line n , on the red side of the spectrum, is

$$f_n = nf_{rep} + f_{ceo} \quad (6)$$

then the corresponding second harmonic comb line, $2n$ on the blue end of the spectrum, will have a frequency

$$f_{2n} = 2nf_{rep} + f_{ceo}. \quad (7)$$

The heterodyne beat between the doubled first harmonic and the single second harmonic frequency will yield a difference frequency which is simply f_{ceo} :

$$2f_n - f_{2n} = 2(nf_{rep} + f_{ceo}) - (2nf_{rep} + f_{ceo}) = f_{ceo}. \quad (8)$$

This self-referencing method represents a tremendous advancement over traditional optical frequency metrology techniques because it makes obsolete the need for any stabilized single-frequency lasers, and requires only a single mode-locked laser [9].

In order to obtain the octave spanning spectrum necessary to exploit the simple self-referencing technique the frequency comb needs to be spectrally broadened. This can be achieved by sending the pulse through an air-silica microstructure fiber [5, 12]. In such an optical fiber, the spectrum of the mode-locked laser is broadened through the nonlinear process of self-phase modulation; however, chromatic dispersion in the fiber stretches pulse duration and thus limits the amount of generated spectra, and external broadening introduces noise which limits the overall stability of the system [9]. Recently, an octave spanning prismless Ti:sapphire laser has been demonstrated, which instead of using silica fiber to broaden the spectrum, employs novel double chirped mirror pairs inside the cavity to broaden the spectrum internally [6].

If an octave spanning spectrum cannot be achieved, one can still use self-referencing techniques to obtain f_{ceo} . If the spectrum is considerably narrower and spans only 2/3 of an octave, one can compare the second and third harmonics ($2f$ -to- $3f$) to produce a measurement of f_{ceo} . However, using higher order harmonics introduces complications with increasing nonlinearity into the system, but the loosened requirement for spectral width does represent a clear advantage [7].

In order to completely stabilize the frequency comb, the second degree of freedom, the pulse repetition rate f_{rep} also needs to be controlled. There are two alternative ways to stabilize the repetition rate of a mode-locked laser. It is possible to lock f_{rep} in the frequency domain to the hyperfine cesium transition frequency, f_{cs} . However, the accuracy of this lock is limited by the extent to which f_{cs} is known to absolute certainty. Any noise in the lock between f_{rep} and f_{cs} in the frequency domain will be amplified a million times in the optical domain, because the optical frequencies are 10^6 times greater than the repetition rate

frequency. Thus locking f_{rep} to f_{cs} as a means to stabilize the comb lines is only a realistic and convenient approach if an extremely stable Cesium reference clock is available. If such an accurate frequency standard is not readily available, it is easier to stabilize the comb by locking the repetition rate f_{rep} to a known optical transition frequency of a cw laser, such as the 1s-2s transition, in the optical domain. Any noise present in the cw laser frequency will then be divided by a factor of 10^6 in the frequency domain. By this method, all comb lines are locked to the 1s-2s transition, which represents a very stable control of the repetition rate, and hence ensures overall control of the frequency comb.

Chapter 3

Description of the System and Experimental Setup

3.1 The System

The system designed to stabilize and measure f_{ceo} consists of two main components: A novel octave spanning prism-less Ti:Sapphire laser used to generate ultrashort pulses on the order of 5 femtoseconds, and an electro-optical feedback system which determines and stabilizes f_{ceo} through the self-referencing $1f$ - $2f$ process described above.

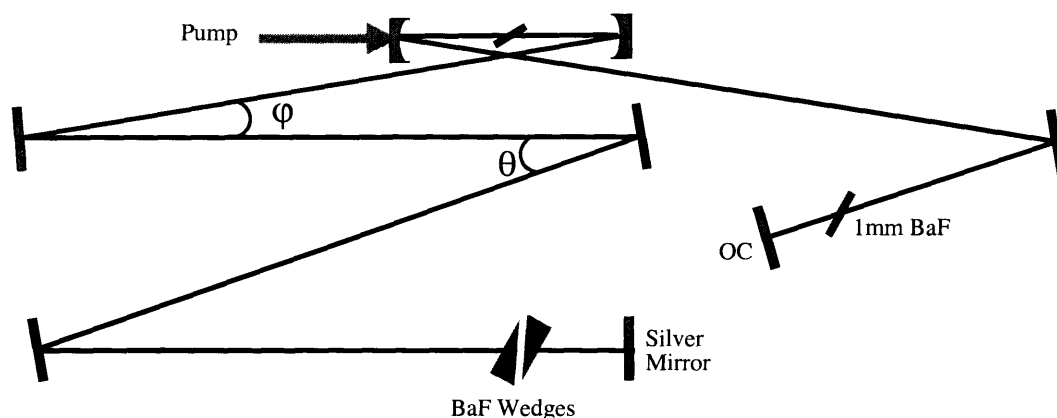


Figure 3-1: Schematic diagram of octave-spanning prism-less laser. Gray and black mirrors are type I and II DCMs respectively. The BaF₂ wedges are used for fine-tuning the dispersion [1].

3.1.1 The Laser

For this experiment, an 80 MHz, octave-spanning Ti:Sapphire laser system built by Matos *et al* at the RLE at MIT, is used [1]. The laser is prism-less and the required broadband dispersion compensation is provided by novel double-chirped mirror pairs in combination

with thin BaF₂ wedges. Precise dispersion compensation over a wide bandwidth is crucial to generate a stable octave spanning spectrum. If prisms are used to provide dispersion compensation, the laser becomes highly sensitive to cavity alignment, thus the prism-less design described here produces greater long-term mode-locking stability [1].

The laser design consists of an astigmatically compensated x-folded cavity and a 2 mm long Ti:Sapphire crystal with an absorption of $\alpha=7 \text{ cm}^{-1}$ at 532 nm. The pump lens has a 60mm focal length and the radius of curvature (ROC) of the folding mirrors is 10 cm. The output power in cw operation is typically 40 mW with 4.4 W pump power, whereas in mode-locked operation, the average power is 90 mW. With the exception of the end mirrors, all mirrors employed in the cavity are type I (gray) and type II (black) double-chirped mirrors (DCM) that generate smooth group delay dispersion when used in pairs; a silver mirror and a broadband output coupler (OC) with a ZnSe/MgF₂ coating giving 1% transmission are used as end mirrors [1].

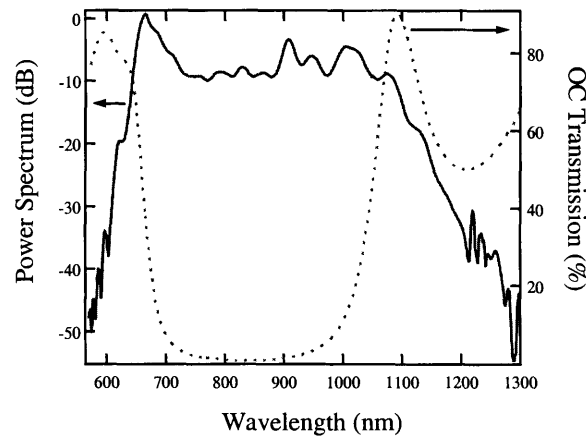


Figure 3-2: Measured output spectrum (solid line) for 80 MHz repetition rate laser. The octave is reached at approximately 25 dB of the average power level. The average mode-locked power is 90 mW. Also shown is the OC transmission curve (dashed line) for the ZnSe/MgF₂ Bragg-stack, which has approximately 1% transmission at 800 nm [1].

The twelve bounces on the DCMs which a laser pulse encounters during one cavity round trip generates the exact amount of negative dispersion required to compensate for positive second and third order dispersion caused by the laser crystal, the air path in the

cavity, and the BaF₂ wedge-pairs used to fine tune the intracavity dispersion [1]. The laser is mode-locked by reducing the amount of BaF₂ inside the laser cavity, and the output spectrum may be broadened by optimizing the insertion level of the BaF₂ wedge. The advantage of using a prism-less laser is that adjusting the dispersion does not significantly affect the cavity alignment, which makes the laser employed very stable, fully operational for up to a day without interruption [1]. The spectrum of the 80 MHz laser is given in Figure 3-3. As can be seen, the octave is reached at a spectral density about 25 dB below the average level.

3.1.2 f_{ceo} Feedback-Control System

So that the broadband mode-locked laser may be employed as a frequency comb generator, it is necessary to control both the carrier-envelope offset frequency, f_{ceo} , and the repetition rate, f_{rep} . By using the technique of self-referencing described in the previous section, f_{ceo} is directly measured. Figure 3-3 describes the feedback control system which was designed by Matos *et al.* to measure and control the carrier-envelope offset frequency [1]. The laser output is split into long and short wavelength components using a dichroic beamsplitter, and recombined after insertion of a proper time delay stage. Because of the difference in group delay of the 580 nm and 1160 nm radiation in the optical components (beamsplitter, OC, and BBO crystal), the delay stage is essential to ensure that the separated beams are recombined in phase. The recombined beam is focused into a 1 mm BBO crystal and sent through a 10 nm wide spectral filter centered at 580 nm. The doubled 1160 nm light and the fundamental 580 nm light are then projected into the same polarization to enable interference, so that the two light beams may both temporally *and* spatially overlap, which is crucial for producing a beat note. The beat signal is detected by a photo multiplier tube (PMT). Control of the comb stability is guaranteed by filtering the component of $f_{rep} + f_{ceo}$ at 130 MHz from the PMT signal and phase-locking to a stable RF synthesizer using a phase-locked loop. To improve the lock, the locking range is increased by filtering and amplifying the 130 MHz component

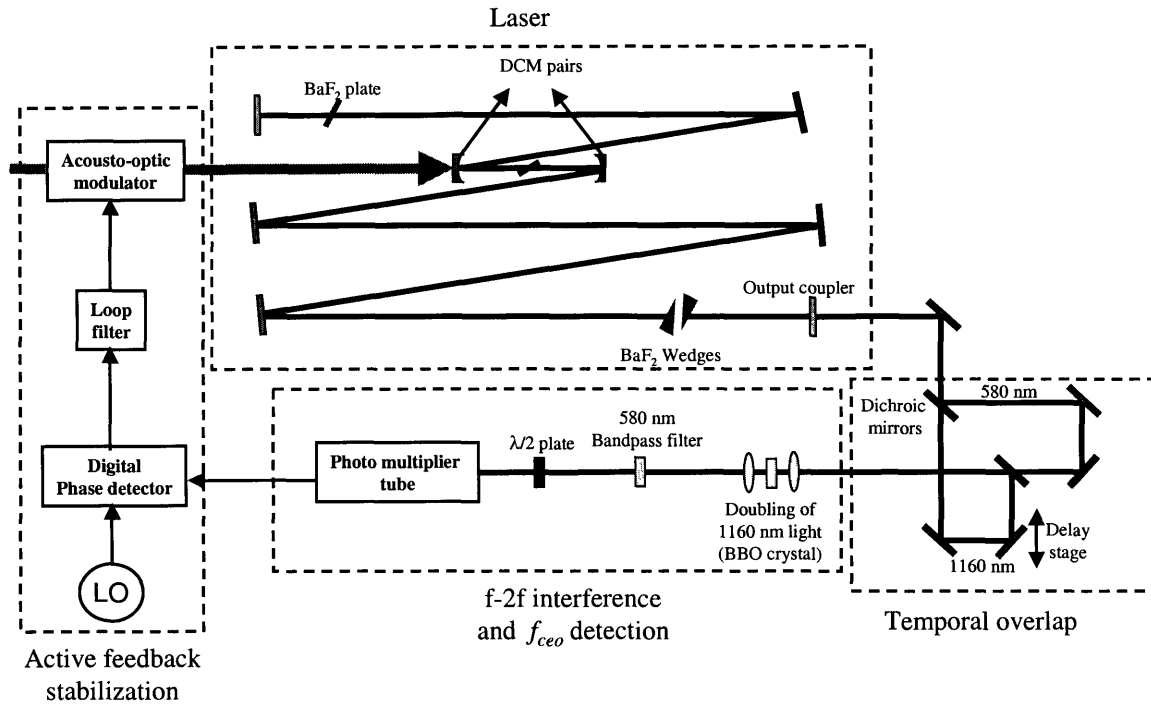


Figure 3-3: Setup for f_{ceo} detection and lock. Main components of the system include the laser itself, the self-referencing f-2f interference setup, and the active feedback and stabilization electronics [1].

of the signal, sending it to a 32-fold frequency divider (this is variable, it can also be a 16-fold), and comparing it with the synthesizer signal in a digital phase detector. The filtered and amplified phase error signal controls the pump power via an acousto-optic modulator, which completely controls the carrier-envelope frequency of the mode-locked laser. This completes the feedback loop. The modulation of the pump power can be used to control f_{ceo} over the required bandwidth, in a prism-less cavity.

3.2 Experimental Setup

The feedback system described above is used to control f_{ceo} and the stability of the frequency comb. In order to be able to use the frequency comb for optical metrology, the integrated phase error of the f_{ceo} beat needs to be less than 2π radians, or else, cycle slips will occur, rendering the comb impractical for our purposes. In order to produce a stable frequency comb, the accumulated phase noise error of the f_{ceo} needs to be minimized. However, phase spectral density measurements have shown that noise in the pump power of the laser directly affects the noise in the carrier-envelope frequency of the mode-locked laser [1]. In order to improve the stability of the frequency comb, a minimization of the pump noise is thus extremely desirable. In addition to the AOM, a commercially manufactured noise eater is placed into the system, which directly cancels the pump power noise through a feedback system.

3.2.1 *The Electro-optical Modulator Noise Eating System*

In the feedback control system used in this experiment, the AOM acts as a transducer which controls the f_{ceo} lock through modulating the pump power. The AOM should be capable of eliminating the pump noise by locking f_{ceo} . This however, is not the case. The feedback control loop employed does not eliminate all the noise of the pump, and some residual noise correlated to pump noise is seen in the f_{ceo} . Thus the noise eater is used to pre-stabilize the

pump, so that f_{ceo} is less noisy to begin with. This device cancels the noise of the pump power in its capacity as an amplitude modulator.

The operation of the noise eater is described in Figure 3-4 (a, b). Before the laser beam is aligned into the aperture of the noise eater, it is passed through a polarizer, to ensure that the incident light is purely vertically polarized (Figure 3-4 (a)). By applying a bias voltage to the electro-optical crystal, the polarization of the laser light is rotated by an angle θ . By subsequently being passed through another polarizer, the vertical component of the light is again filtered out (the horizontal component is rejected and emitted through the polarizer escape port), however, its intensity has been reduced to $I \cos^2 \theta$.

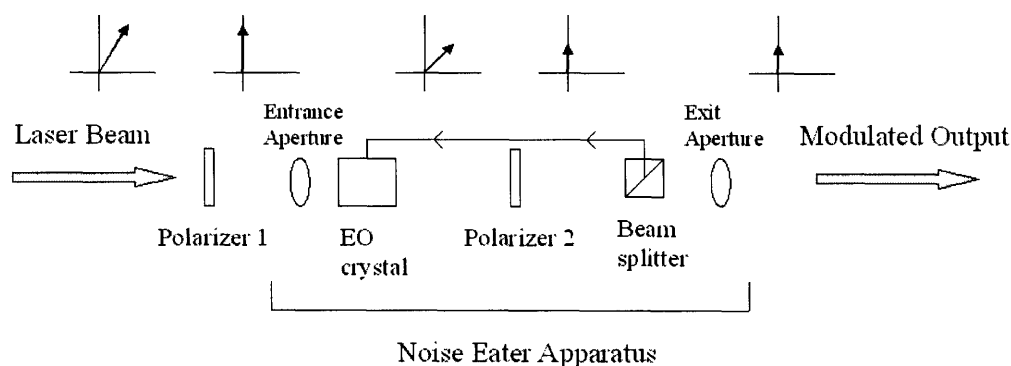


Figure 3-4 (a): The Noise Eater apparatus. Note that the Electro-optical crystal is a polarization rotator.

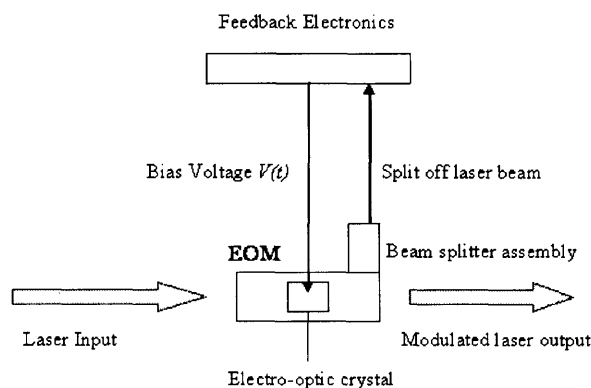


Figure 3-4 (b): The Noise Eater feedback system. The detected signal from the beam splitter is compared to a reference signal in the feedback electronics, and a bias voltage is applied to the electro-optic crystal.

A percentage of this reduced intensity signal is then split off by a beam splitter assembly, which consists of an attenuating polarizer and a photodiode preamp, and sent via an optical fiber to the feedback electronics, where it is compared to an internally produced reference signal. The difference between the detected signal and an internal reference causes an amplifying signal to be applied to the modulator 180 degrees out of phase with the original detected signal, as a result of which the amplifier tries to reduce the differential errors existing at its input[13]. This feedback loop effectively cancels the pump noise of the system.

Thus the noise eater's operation critically depends on two voltages. The bias voltage is applied to the crystal to initially change the polarization by a substantial amount, which is essential to ensuring that subsequently the feedback signal may reduce the pump noise by either increasing or decreasing the polarization. The DC signal voltage then applied to the crystal as part of the feedback loop changes the polarization by the incremental amount necessary to cancel the noise effectively.

To test the functionality of the EOM noise eating system, the following setup is used (Figure 3-5). The laser beam is passed through a wave-plate to allow for polarization adjustments. Before being aligned into the EOM, the laser beam is directed along a set of silver mirrors, to allow for optimization of the beam through the EOM. The transmitted laser beam is then measured and characterized alternately on a power meter or an oscilloscope by aiming it at a photodiode. The EOM itself is mounted on the optical table in such a way that it may easily be rotated, to allow for optimum roll adjustment. It is further placed on a platform which allows for pitch and yaw adjustments. These fine adjustments are essential for ensuring that the transmission through the EOM can be maximized. Lastly, in front of the pair of folding mirrors used to align the beam into the EOM aperture, an iris is placed. This iris is used to control the beam size, and useful for investigating what the optimum aperture of the EOM should be for maximizing laser beam transmission. The photodiode signal is then measured on a Vector Signal Analyzer, Agilent Model No.89410 A. This device measures

the noise spectral density of the input laser power by performing a Fast Fourier Transform (FFT) of the signal.

The set up is constructed in such a way that upon passing through the EOM, the laser beam may be redirected onto its original path through the laser cavity, so that as a future experiment, the laser may be run and locked with the EOM in place, and the f_{ceo} phase noise determined.

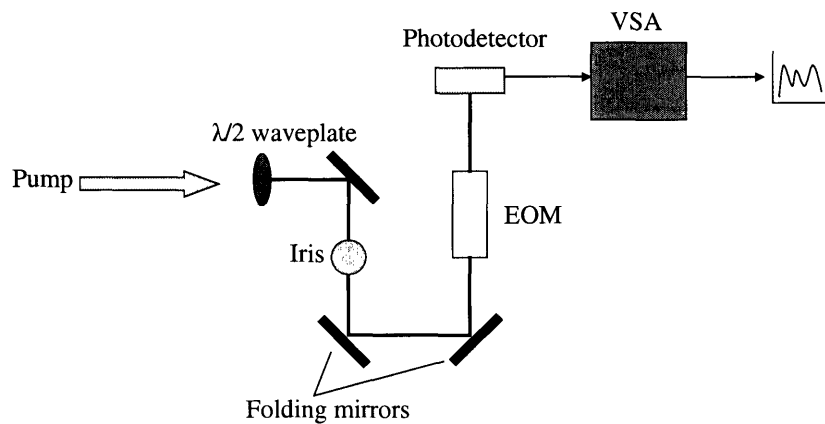


Figure 3-5: The experimental set up for testing the EOM performance as a pump power noise eater. The half-waveplate is used to make polarization adjustments. The pair of folding mirrors in front of the EOM is used for optimization of the laser beam transmission through the EOM.

Chapter 4

Measurements and Results

4.1 Noise reduction

In this experiment we measure the pump noise of the laser by using a Vector Signal Analyzer. Since it has been shown that pump noise is directly correlated to phase noise in the f_{ceo} , stabilizing the pump power should reduce the accumulated phase noise of the f_{ceo} . Measurements of the spectral densities of the phase error signals for the locked f_{ceo} and the pump noise laser are shown in Figure 4-1.

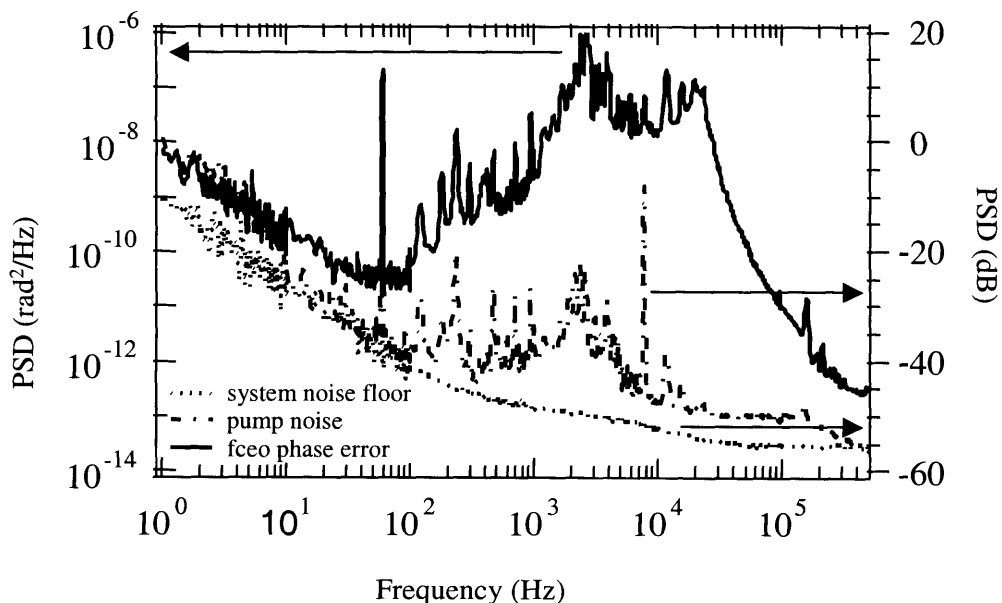


Figure 4-1: Spectral densities of the phase error signal at the output of the digital phase detector for the f_{ceo} lock (solid line) with scale on the left. Spectral density of the pump noise (dash-dotted line) and system noise floor (dotted line), with scale on the right. The major contribution to f_{ceo} noise is due to pump noise [1].

The correlation between pump noise and phase noise in the f_{ceo} can be clearly discerned from this measurement. Note that the pump noise measurement was taken in the absence of f_{ceo} feedback. Because of the limited bandwidth of the AOM, it is not possible to suppress all of the pump noise, and hence improve the overall quality of the f_{ceo} lock, with it. Thus, we add the noise eater, as described in the previous section, to pre-stabilize the pump and measure its pump noise reduction capabilities. First, transmission through the EOM is optimized, and a maximum of 78% without the beamsplitter attached is observed. A corresponding extinction ratio of 66:1 is measured. Although this is far from the optimal of 100:1, it suffices for the purposes of this noise measurement. Adjusting the bias voltage correctly further ensures that the maximum amount of laser light is transmitted, and minimizes the rejected polarization component which is ejected through the polarizer escape port of the EOM. The beamsplitter assembly is calibrated so that the signal detected by the feedback electronics is physically meaningful. The laser power is set to 1 W. While this is only a fraction of the actual operating power of the laser when the system is running, higher powers are avoided to prevent possible damage to the EOM, even though the EOM we are using is classified as a high power version. The Vector Signal Analyzer used for making the phase noise measurements is AC coupled at 50 Ω and 3 averages per decade are recorded.

Measurements of the free running pump noise, the noise level of the free running pump after implementation of the EOM, as well as the system's noise floor are given in Figure 4-2. As can be seen, because of the EOM's increased bandwidth compared to the AOM, it is able to reduce the pump noise of the laser by the substantial amount of 20 dB over almost the entire range of frequencies. Most importantly, the noise eater effectively cancels the noise in the frequency range relevant for the experiment, 100 Hz to 10 MHz. A sharp oscillation at 60 Hz is observed both without and with the EOM in operation.

The noise eater's performance could not be tested when the laser was actually mode-locked. However, the reduction in the f_{ceo} noise produced by using the noise eater to pre-

stabilize the pump can be inferred from the accumulated phase noise measurements. Since the f_{ceo} behaves linearly with the pump noise, a reduction of the integrated pump noise should translate to a reduction of the measured f_{ceo} noise. By integrating the noise spectral density over the range of frequencies, we calculate a reduction in the pump noise by a factor of 35 when the noise eater is in operation. Previous measurements showed an accumulated phase error in the stabilized f_{ceo} of 1.4 radians [1]. Therefore it is reasonable to expect that the accumulated phase noise error of the f_{ceo} with the noise eater in operation should decrease to 0.04 radians. This remains to be verified in a future experiment.

As a final measurement, the AOM was replaced with a second EOM, to test if an EOM could also be used in the capacity of a transducer. However, because the aperture of the EOM was too small, the transmission of the laser beam through the EOM was less than satisfactory and no conclusive measurements could be made.

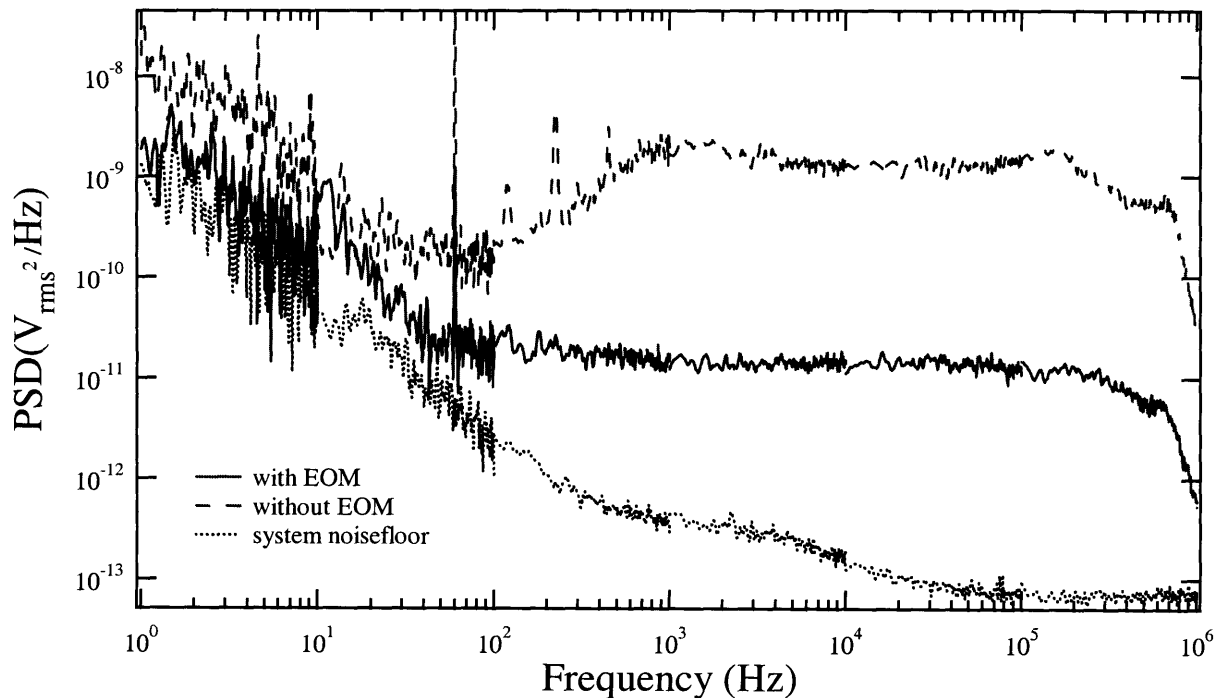


Figure 4-2: Spectral Density Measurements of the Pump Noise without (dashed line) and with (solid line) the EOM in operation. The dotted line is the system noise floor.

4.2 Beam Characterization

In order to effectively use the Noise Eater, the transmission of the laser beam through the EOM and its electro-optic crystal and beamsplitter components needs to be maximized. Also, maximizing the transmission simultaneously optimizes the extinction ratio of the EOM and ensures optimum performance and noise cancellation. Furthermore, undistorted transmission of the beam is crucial, because the Ti:Sapphire laser operation depends critically on the quality of the pump beam profile. Because the EOM used in this experiment has an aperture of 3 mm, and the laser beam $1/e^2$ beam waist is 2.6 mm, it is tremendously difficult to transmit the beam undistorted through the EOM. When the EOM is carefully adjusted in pitch, yaw and roll, the maximum power transmission that can be achieved at full beam size is 75%, but the quality of the transmitted mode is distorted. Most of the time, the exiting beam profile is distorted, exhibiting either a square or an elliptical profile. Thus the 2.6 mm beam must be too large for the 3 mm aperture, and incidentally must be clipping at its edges while it travels through the EOM. It is also observed that with increasing power, the transmission improves. Upon investigating the relationship between power level and beam size by means of a beam profiler, we discover that with increasing power, the beam waist becomes smaller. Thus, with increasing power, and hence decreasing beam size, the power transmission through the EOM improves (Figure 4-3). Hence, this lends further proof to the assumption that the actual natural beam size is simply too large to be transmitted through the EOM in an undistorted fashion.

Thus to determine what the optimum beam size should be for maximizing transmission, and hence, also to optimize effective noise cancellation, transmission and beam size are measured systematically at a constant power of 0.5 W. The beam size is controlled by means of an iris, which allows for a very gradual adjustment of beam diameter. Since the beam is assumed to have a gaussian profile, care is taken to ensure that it is centered exactly on the iris. Because the iris is not a perfect pinhole, except when it is virtually all the way

closed, the recorded beam profiles for the partially closed iris stages are not ideally circular, but instead appear heavily distorted. However, a systematic gradual reduction of the beam size while holding the power constant lets us determine the maximum beam waist allowed. Defining beam quality as (incident beam size)/(exiting beam size), 100% would indicate that the beam passes through the EOM completely undistorted. Thus, when at a certain beam power transmission, the beam size becomes small enough for the beam to be transmitted in its entirety, we would expect the graphs of the decreasing beam size to converge. This is in fact the case (Figure 4-5). Plotting both beam size without the EOM and with the EOM as a function of power transmission through the EOM, the graphs converge at a power transmission of 69% and a beam diameter of 1050 μm . Thus when pumping at 0.5 W of power, the maximum beam size for optimal EOM noise reduction is a diameter of 1050 μm .

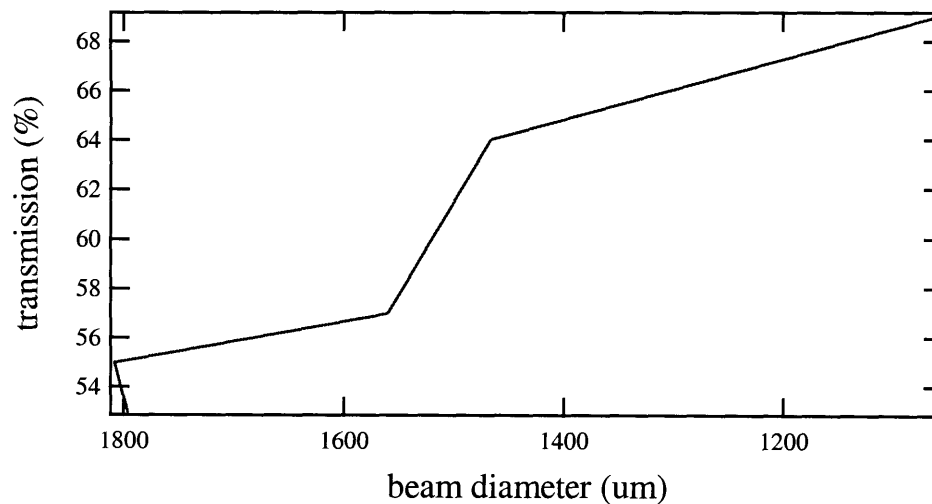


Figure 4-3: Transmission of power through the EOM as a function of beam size. Clearly, as the beam size becomes smaller, more power can be transmitted through the EOM, indicating that the beam is no longer distorted or clipping because it is too large for the aperture.

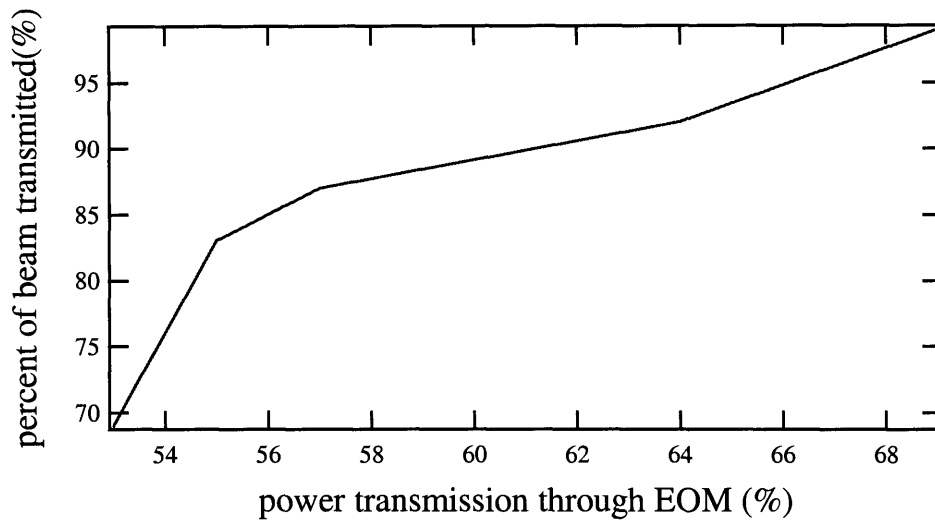


Figure 4-4: Beam size transmission as a function of power transmission. As the EOM transmits a higher percentage of the incident power, the quality of the laser beam transmitted, defined by incident beam size/exiting beam size, also improves

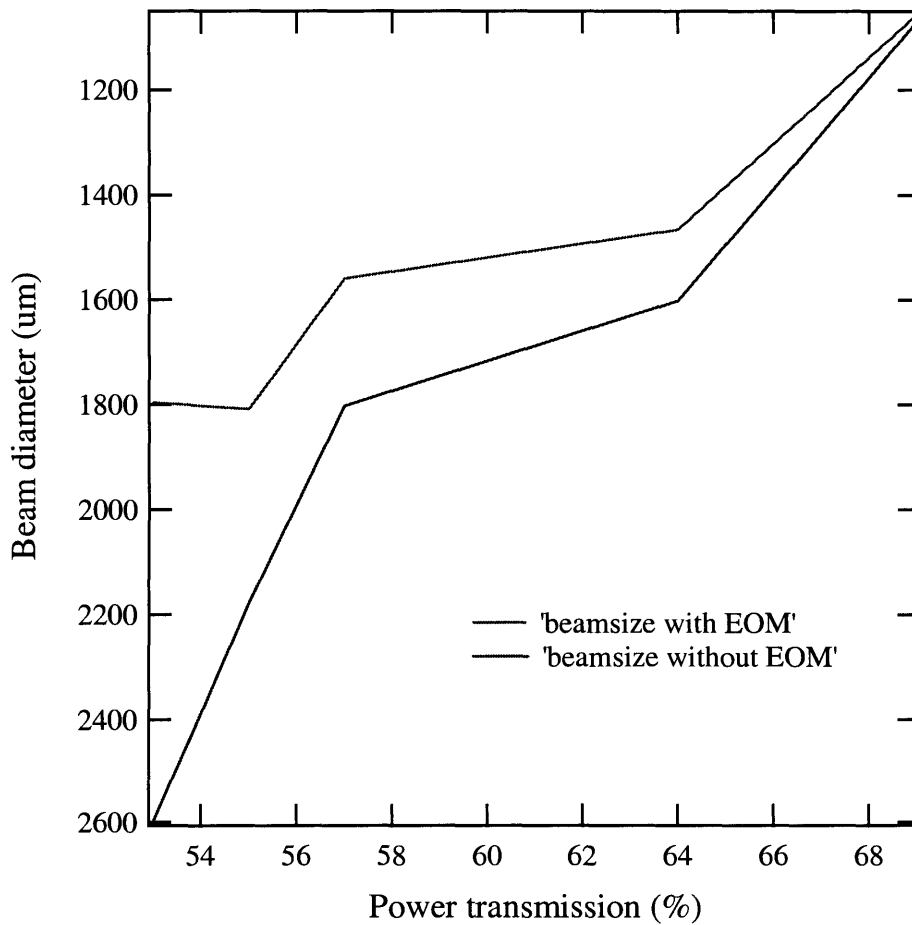


Figure 4-5: Graphical estimate of the maximum beam size for optimum EOM operation at a power of $\frac{1}{2}$ W.

Chapter 5

Conclusion and Future Research

This thesis investigated the possibility of employing a commercially manufactured noise eater system to reduce f_{ceo} phase noise of a prism-less octave spanning Ti:Sapphire laser by pre-stabilizing the pump power. The noise eater is demonstrated to effectively reduce the pump noise by 20 dB over a wide range of frequencies. Although a direct measurement of f_{ceo} noise with the noise eater in operation could not be made, the reduction of f_{ceo} phase noise can be inferred from integrated pump phase noise measurements. Furthermore, this thesis investigated the optimal beam size for the noise eater to work effectively, and demonstrated that the aperture of the noise eater being used was too small for ideal operation.

It is calculated that the noise eater is capable of reducing the pump noise by a factor of 35. If this pump noise reduction translates linearly to a reduction of f_{ceo} noise, an assumption supported by measurements of pump noise and f_{ceo} noise, the noise eater could be used to greatly improve the overall stability of the frequency comb. The logical next step is to utilize a noise eater model of appropriately large aperture (5 mm, as opposed to 3 mm), and to lock f_{ceo} with the overall goal of producing a frequency comb stable enough to utilize in high precision optical metrology.

References

- [1] L. Matos *et al.*, “Direct frequency comb generation from an octave-spanning, prism-less Ti:Sapphire laser,” Accepted for publication in Optics Letters.
- [2] L.-S. Ma *et al.*, Phys. Rev. A **64**, 021802(R) (2001).
- [3] R. K. Shelton *et al.*, Science **293**, 1286 (2001).
- [4] J. Ye *et al.*, Phys. Rev. Lett. **87**, 270801 (2001).
- [5] J. Reichert *et al.*, Opt. Comm. **172**, 59-68 (1999).
- [6] F. X. Kärtner *et al.*, J. Opt. Soc. Am. B **18**, 882-885, (2001).
- [7] S. T. Cundiff and F. Krausz, “Carrier-Envelope Phase of Ultrashort Pulses”, to appear in “Strong Field Laser Physics,” T. Brabec and H. Kapteyn, eds. (Springer).
- [8] T. M. Fortier *et al.*, Opt. Lett. **27**, 1436-1438 (2002).
- [9] D. J. Jones *et al.*, Science **288**, 635-639 (2000).
- [10] L. Xu *et al.*, Opt. Lett. **21**, 2008 (1996).
- [11] Th. Udem *et al.*, Phys. Rev. Lett. **79**, 2646 (1997).
- [12] J. Ranka *et al.*, Opt. Lett. **25**, 25 (2000).
- [13] Theory of Operation. Conoptics LASS II operations manual.